

Stringent bounds on HWW and HZZ anomalous couplings with quantum tomography at the LHC

M. Fabbrichesi^a, R. Floreanini^a, E. Gabrielli^{b,a,c,d} and L. Marzola^d

(a) *INFN, Sezione di Trieste, Via Valerio 2, I-34127 Trieste, Italy*

(b) *Physics Department, University of Trieste, Strada Costiera 11,
I-34151 Trieste, Italy*

(c) *CERN, Theoretical Physics Department, Geneva, Switzerland*

(d) *Laboratory of High-Energy and Computational Physics, NICPB, R vala 10,
10143 Tallinn, Estonia*

ABSTRACT

Quantum tomography provides the full reconstruction of the density matrix of a state. We use it to study the Higgs boson decay into weak gauge bosons. Anomalous couplings beyond the Standard Model can be constrained by means of observables easily defined in terms of the polarization density matrix. We describe a strategy based on three observables that together provide the most stringent limits. Two of these observables are linked to the entanglement between the polarizations of the two gauge bosons, the other is based on CP-odd combinations of one momentum and two polarizations. We find for the Z channel that this strategy offers, already with the available LHC data, limits competitive with the best available bounds. We argue that the inclusion of these observables in routine experimental analyses can lead to more stringent global fit limits.

⊠

1 Introduction

THE DECAY OF THE HIGGS BOSON provides an ideal laboratory for a systematic study of weak gauge bosons polarizations. The massive gauge bosons—whose polarizations represent quantum states with three possible levels, that is, *qutrits*—act as their own polarimeters and the full polarization density matrix can be reconstructed, within the inherent uncertainties of the procedure, from the angular distribution of the final leptons in what has been dubbed *quantum tomography*.

This opportunity has been explored in a series of papers [1–4] in which the polarization density matrix of the bipartite system formed by the two gauge bosons has been computed, and observables quantifying the *entanglement* [5] and the violation of the Bell inequalities [6] were analyzed.

In this work we utilize the polarization density matrix of the processes $H \rightarrow WW^*$ and $H \rightarrow ZZ^*$ (where W^* and Z^* denote off-shell states) to study the effect of possible anomalous couplings between the Higgs boson and the weak gauge bosons. The study of anomalous couplings is an important area of research in particle physics because their existence would imply the presence of new particles or interactions. Their precise measurement can then provide insights into the nature of new physics beyond the Standard Model (SM). We are particularly interested in the CP nature of these couplings and the related question of the parity of the Higgs boson, that is, whether it has or not a pseudo-scalar component.

The most general Lagrangian for the processes we are interested in can be written as

$$\begin{aligned} \mathcal{L}_{HVV} = & g M_W W_\mu^+ W^{-\mu} H + \frac{g}{2 \cos \theta_W} M_Z Z_\mu Z^\mu H \\ & - \frac{g}{M_W} \left[\frac{a_W}{2} W_{\mu\nu}^+ W^{-\mu\nu} + \frac{\tilde{a}_W}{2} W_{\mu\nu}^+ \tilde{W}^{-\mu\nu} + \frac{a_Z}{4} Z_{\mu\nu} Z^{\mu\nu} + \frac{\tilde{a}_Z}{4} Z_{\mu\nu} \tilde{Z}^{\mu\nu} \right] H, \end{aligned} \quad (1.1)$$

The first line in Eq. (1.1) gives the SM Lagrangian, the second introduces two possible anomalous couplings for each of the gauge bosons $V = W$ or Z : a_V and \tilde{a}_V . In Eq. (1.1), g is the $SU(2)$ coupling, $V^{\mu\nu}$ are the field strength tensors and $\tilde{V}^{\mu\nu} = \frac{1}{2} \epsilon^{\mu\nu\rho\sigma} V_{\rho\sigma}$. All couplings in Eq. (1.1) are taken to be real. The coupling a_V stands for a departure of the fundamental interaction from that of the SM. A non-vanishing coupling \tilde{a}_V signals the presence of a pseudo-scalar component in the Higgs boson and the possibility of CP violation in the interference with the SM vertex.

Numerous works have studied the anomalous couplings in Eq. (1.1) by means of dedicated observables [7–17] and in the framework of effective field theories [18–20]—even though most of the references only consider observables that are combinations of the final lepton momenta and energies. The structure of the helicity amplitudes for the considered processes has been investigated in [21–27] and applied to the anomalous couplings in [28].

In this work, we introduce a new strategy that exploits the full polarization density matrix. Knowledge of the density matrix gives a bird’s-eye view of the possible observables available for a given process. Some of them, like those linked to entanglement, are untested yet. Others are already known and utilized, like products of momenta and polarizations or the cross section—the simplest of them all.

For the present case of the Higgs boson decays, we define three observables in terms of the entries of the polarization density matrix to provide a new mean to constrain the anomalous couplings in Eq. (1.1): two observables are linked to entanglement in the spin correlations, the third is related to products of one momentum and two polarizations and it is specific to the CP-odd vertex. This combination of observables seems as sensitive or even more to any changes in the Lagrangian as analyses based on data from multiple cross sections and, therefore, it represents a useful tool to further build on this more traditional approach.

Polarizations are more difficult to measure than momenta. The reconstruction of the polarization density matrix from the data is challenging, in particular for the case of $H \rightarrow WW^*$ because of the presence of the undetectable neutrinos. The main aim of this work is to show that the extra work needed to reconstruct the gauge boson polarizations is indeed worthwhile. In order to present an analysis as realistic as possible, we give an estimate of the main uncertainties in the bounds that we derive for the anomalous couplings. In particular, we include the effects of statistical and systematic errors, as well as the impact of the dominant irreducible backgrounds in the computation of these observables. It is understood that a complete treatment of uncertainties goes beyond the purpose of the present work and should be the focus of a dedicated analysis that can only be performed by the experimental collaborations.

To assess how our method fares, we compare the bounds we derive with the theoretical analysis presented in [28]. Comparison with experimental limits requires the inclusion of the irreducible background. We estimate this for the ZZ^* channel, which achieves a higher sensitivity, and confront our findings with the limits due to a combination of cross sections recently updated the CMS [29] collaboration.

2 Methods

QUANTUM TOMOGRAPHY aims to fully determine the density matrix ρ of a quantum state. In the case of the decay of the Higgs boson into two massive spin 1 gauge bosons, the density matrix for the joint polarization states of the two particles is the 9×9 matrix of a system composed by two qutrits. It can be decomposed on the basis formed by the eight Gell-Mann matrices T^a and the unit matrix as follows

$$\rho_H = \frac{1}{9} [\mathbb{1} \otimes \mathbb{1}] + \sum_a f_a [T^a \otimes \mathbb{1}] + \sum_a g_a [\mathbb{1} \otimes T^a] + \sum_{ab} h_{ab} [T^a \otimes T^b] \quad (2.1)$$

where the T^a satisfy the orthogonality condition $\text{Tr}[T^a T^b] = 2\delta^{ab}$ and the indices λ and λ' track the polarizations of the two spin 1 massive particles. Eq. (2.1) defines the coefficients f_a , g_a , and h_{ab} ($a, b \in \{1, \dots, 8\}$) which we determine in what follows.

To best constrain the anomalous couplings in the Lagrangian Eq. (1.1), we need observables that ideally depend linearly on these quantities. Quantum tomography gives the coefficients f_a , g_a , and h_{ab} of the density matrix and there is a number of observables that can be constructed with them. Some of these observables are novel and based on the entanglement between the final states, others are linked to correlations already studied or, directly, to the cross section of the process. We consider the three that provide the most stringent limits to the anomalous couplings:

- When a scalar particle decays into a pair of massive gauge bosons, the qutrits describing the polarizations of the latter form a bipartite pure state. In this case it is possible to quantify the entanglement among the polarizations of the weak gauge bosons by computing the *entropy of entanglement*, \mathcal{E}_{ent} , defined by

$$\mathcal{E}_{ent} = -\text{Tr}[\rho_A \log \rho_A] = -\text{Tr}[\rho_B \log \rho_B], \quad (2.2)$$

where ρ_A and ρ_B are the reduced density matrix obtained by tracing out the subsystem B or A , respectively. In our case, the two subsystems are the polarizations of the two massive gauge bosons and the reduced density matrices are obtained by tracing out the polarizations of either gauge boson. For a two-qutrit system the entropy of entanglement satisfies $0 \leq \mathcal{E}[\rho] \leq \ln 3$.

The first equality is true if and only if the bipartite state is separable (signalling the absence of entanglement), the second if the bipartite state is maximally entangled;

- The second observable \mathcal{C}_2 [30] is an entanglement witness defined in terms of the coefficients in Eq. (2.1) as

$$\begin{aligned} \mathcal{C}_2 = & 2 \max \left[0, -\frac{2}{9} - 12 \sum_a f_a^2 + 6 \sum_a g_a^2 + 4 \sum_{ab} h_{ab}^2, \right. \\ & \left. -\frac{2}{9} - 12 \sum_a g_a^2 + 6 \sum_a f_a^2 + 4 \sum_{ab} h_{ab}^2 \right]. \end{aligned} \quad (2.3)$$

It represents a lower bound on the *concurrence* [31] of the system, which quantifies the entanglement of a generic bipartite system. Unfortunately, the definition of concurrence is based on an optimization problem that makes its evaluation a very hard mathematical task—with a simple analytic solution only when the two subsystems are two-level systems (qubits). For this reason, we use \mathcal{C}_2 as proxy for the concurrence. Whereas the entropy of entanglement can be used to quantify the entanglement content only of pure states, the observable \mathcal{C}_2 can be utilized for arbitrary states. \mathcal{C}_2 is at most equal to $4/3$.

- The third observable \mathcal{C}_{odd} singles out the asymmetric parts of the density matrix; it defined as

$$\mathcal{C}_{odd} = \frac{1}{2} \sum_{\substack{a,b \\ a < b}} |h_{ab} - h_{ba}|, \quad (2.4)$$

which contains only off-diagonal terms that change sign under transposition. In the difference symmetric terms drop out. The combinations in Eq. (2.4) provide correlations. They can be written in terms of the kinematical variables as triple products of momenta and polarizations as, for instance,

$$\vec{k} \cdot (\vec{\varepsilon}_{\hat{n}} \times \vec{\varepsilon}_{\hat{r}}), \quad (2.5)$$

with \vec{k} the momentum of one of the particles, $\vec{\varepsilon}_{\hat{n}}$ and $\vec{\varepsilon}_{\hat{r}}$ the projections of the polarizations along two directions orthogonal to the momentum.

The decay of the Higgs boson shows at colliders in the processes

$$p p \rightarrow V_1 + V_2 + X \rightarrow \ell^+ \ell^- \text{ (or } \ell^+ jj \text{ or } \ell^- jj) + E_T^{\text{miss}} \text{ (or } \ell^+ \ell^-) + \text{jets}, \quad (2.6)$$

with missing energy E_T^{miss} due to the possible presence of neutrinos in the final state. These processes include the production of the gauge bosons through the resonant Higgs boson channel, as well as via quark fusion, and include the consequent decays into the final leptons or quarks—plus the jets originating from the spectator quarks.

The production of the Higgs boson is dominated at the LHC by gluon fusion. This is the mode we study. Sub-leading, but not negligible, electroweak processes like vector boson fusion (VBF) contribute as well. In these processes the anomalous couplings enter off-shell. Some of the new physics vertices are enhanced by the energy and make some of these off-shell contribution more sensitive. Moreover, they may enter twice, first in production and then in the decays. For these reasons, comparison of bounds obtained from different processes as well as a direct comparison of our bounds to others is often not straightforward.

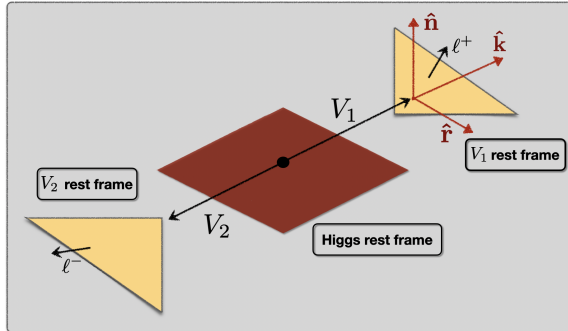


Figure 1: Unit vectors and momenta utilized in the text to describe the decay of the Higgs boson into the weak gauge bosons V_1 and V_2 .

The spin 1 gauge bosons act as their own polarimeters and the momenta of the final leptons (see Fig.1) provide a measurement of the gauge boson polarizations. The quantum tomography problem of reconstructing the correlation coefficients h_{ab} , f_a and g_a from the final states of the process at hand has been recently discussed in [3], to which we refer for more details.

In the case of the Higgs boson decay, the computation of the correlation coefficients is greatly simplified because there are only two independent entries in the density matrix that need to be determined. All the elements of the density matrix can be written either in terms of the Gell-Mann basis or of that of the helicity amplitudes:

$$h_\lambda = \langle V(\lambda)V^*(-\lambda) | -\mathcal{L} | H \rangle \quad \text{with} \quad \lambda = 0, \pm, \quad (2.7)$$

with \mathcal{L} the Lagrangian given in Eq. (1.1). Helicities are here defined with respect to the \hat{z} direction in the rest frame of the first spin-1 particle.

2.1 Estimating the uncertainty

In order to evaluate the sensitivity of the experiments to the anomalous couplings in the observables \mathcal{E}_{ent} , \mathcal{C}_2 and \mathcal{C}_{odd} , we first estimate the number of suitable events which are available.

The cross sections (at $\sqrt{s} = 13$ TeV) of the two processes we are interested in are

$$\sigma(pp \rightarrow H \rightarrow W^+ \ell^- \bar{\nu}_\ell) = 12.0 \pm 1.4 \text{ pb} \quad [32] \quad (2.8)$$

and

$$\sigma(pp \rightarrow H \rightarrow Z \ell^+ \ell^-) = 1.34 \pm 0.12 \text{ pb} \quad [33]. \quad (2.9)$$

These numbers must be multiplied by the corresponding branching ratios. Among the leptonic ones, we only retain those into electrons and muons. In both cases we have a sufficient number of events to compute the polarizations of the gauge bosons, of the order of 10^5 at the LHC run2 for the WW^* process and roughly 10^3 for the ZZ^* process.

As it is often the case, the definition of better observables from the theoretical point of view goes hand in hand with a more challenging reconstruction of the same from the data.

We take into account the problem of the irreducible uncertainties in the evaluation of the operators for the decays of the WW^* by considering the semi-leptonic decay $H \rightarrow jj\ell\nu_\ell$ (rather than the fully leptonic one) and use the momentum from the s -jet (identified via the c -tagging of the companion jet) to measure the polarization of one of the two W -bosons. It has been shown that the efficiency

of the jet tagging and the decreased uncertainty in the single neutrino momentum may improve the polarization reconstruction [34].

The uncertainty on each of the observables considered, let us call them $O(a_V, \tilde{a}_V)$, is found by the following procedure. The main source of uncertainty comes from the determination of the polarizations and it originates in the reconstruction of the rest frame of the decaying Higgs boson. The same reconstruction is also necessary in the determination of the Higgs boson mass m_H from the events in which the Higgs boson decays into either ZZ^* or WW^* ; we therefore can use the related reconstruction error as a proxy for the dominant uncertainty in our computations. We propagate the uncertainty on the value of m_H to the operators by means of a Monte Carlo simulation, obtaining the related variances σ_i^2 for each of the considered decays as m_H is randomly varied within its experimental uncertainty. This uncertainty includes both statistical and systematic errors.

The procedure works well for the ZZ^* case where it is found that $m_H = 124 \pm 0.18 \pm 0.04$ [35]. For the WW^* channel, only the transverse mass can be determined, and that comes with an error (1σ) of about 5 GeV for the fully leptonic decays [36]. We make here an educated guess by taking half of this uncertainty in the case of the semi-leptonic decays (for which the transverse mass is in addition closer to m_H).

To constrain the values of the anomalous couplings a_V and \tilde{a}_V we introduce a χ^2 test set for a 95% CL

$$\sum_i \left[\frac{O_i(a_V, \tilde{a}_V) - O_i(0, 0)}{\sigma_i} \right]^2 \leq 5.991, \quad (2.10)$$

in which we set the uncertainties σ_i as discussed above. The choice of operators utilized in the test depends on the purity of the WW^* and ZZ^* states as clarified below.

3 Results

CONSIDER THE DECAY

$$H \rightarrow V(k_1, \lambda_1) V^*(k_2, \lambda_2), \quad (3.1)$$

with V either W or Z , and V^* regarded as an off-shell vector boson. Here k_1 and k_2 denote the associated particle momenta and the helicities $\lambda_{1,2}$ take values $\lambda_{1,2} = \{+1, 0, -1\}$.

In the following, we treat the latter as an on-shell particle characterized by a mass

$$M_V^* = f M_V \quad (3.2)$$

reduced by a factor $0 < f < 1$ with respect to the original mass M_V . From the Lagrangian in Eq. (1.1), the amplitude of the Higgs boson decay (3.1) is given by

$$\mathcal{M}(\lambda_1, \lambda_2) = M_{\mu\nu} \varepsilon^{\mu*}(k_1, \lambda_1) \varepsilon^{\nu*}(k_2, \lambda_2), \quad (3.3)$$

with

$$M^{\mu\nu} = g M_V \xi_V g^{\mu\nu} - \frac{g}{M_W} \left[a_V (k_1^\nu k_2^\mu - g^{\mu\nu} k_1 \cdot k_2) + \tilde{a}_V \varepsilon^{\mu\nu\alpha\beta} k_{1\alpha} k_{2\beta} \right], \quad (3.4)$$

where g is the weak coupling, $\xi_W = 1$, and $\xi_Z = 1/(2c_W)$, with $c_W = \cos \theta_W$ and θ_W the Weinberg angle. From the amplitude in Eq. (3.3) we obtain

$$\mathcal{M}(\lambda_1, \lambda_2) \mathcal{M}(\lambda'_1, \lambda'_2)^\dagger = M_{\mu\nu} M_{\mu'\nu'}^\dagger \mathcal{P}_{\lambda_1 \lambda'_1}^{\mu\mu'}(k_1) \mathcal{P}_{\lambda_2 \lambda'_2}^{\nu\nu'}(k_2). \quad (3.5)$$

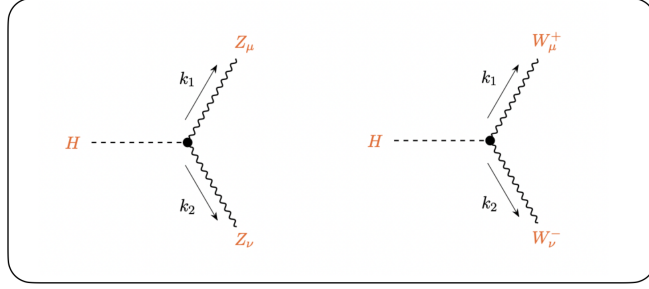


Figure 2: Feynman diagrams for the decay of the Higgs boson into a pair of gauge bosons, the vertex includes the anomalous couplings in Eq. (1.1).

where $\mathcal{P}_{\lambda\lambda'}^{\mu\nu}(k)$ is equal to [37, 38]

$$\begin{aligned} \mathcal{P}_{\lambda\lambda'}^{\mu\nu}(p) &= \varepsilon^\mu(p, \lambda)^* \varepsilon^\nu(p, \lambda') \\ &= \frac{1}{3} \left(-g^{\mu\nu} + \frac{p^\mu p^\nu}{M_V^2} \right) \delta_{\lambda\lambda'} - \frac{i}{2M_V} \varepsilon^{\mu\nu\alpha\beta} p_\alpha n_\beta^i (S_i)_{\lambda\lambda'} - \frac{1}{2} n_i^\mu n_j^\nu (S_{ij})_{\lambda\lambda'} , \end{aligned} \quad (3.6)$$

with S_i , $i \in \{1, 2, 3\}$, being the spin-1 matrix representations of the $SU(2)$ generators. The matrices S_{ij} are defined as $S_{ij} = S_i S_j + S_j S_i - \frac{4}{3} \mathbb{1} \delta_{ij}$, with $i, j \in \{1, 2, 3\}$ and $\mathbb{1}$ being the 3×3 unit matrix. Eq. (3.6) with $M = M_V$ or $M = M_V^*$ for the on-shell and off-shell boson, respectively.¹

By using the expression in Eq. (3.5) we have that

$$\rho_H = \frac{\mathcal{M}_{\mu\nu} \mathcal{M}_{\mu'\nu'}^\dagger}{|\overline{\mathcal{M}}|^2} \left[\mathcal{P}^{\mu\mu'}(k_1) \otimes \mathcal{P}^{\nu\nu'}(k_2) \right], \quad (3.8)$$

where the expression for $\mathcal{P}^{\nu\nu'}(k_{1,2})$ is given in Eq. (3.6) and $|\overline{\mathcal{M}}|^2$ stands for the unpolarized square amplitude of the process, that for $V = W$ reads

$$|\overline{\mathcal{M}}|^2 = \frac{g^2}{4f^2 M_V^2} \Phi_H, \quad (3.9)$$

which in turn gives the cross section. The coefficients f_a, g_a, h_{ab} in Eq. (2.1) can be obtained from the relation in Eq. (3.8) upon a projection of the spin matrices S_i and their products on the Gell-Mann basis [4]. The matrix ρ_H above satisfies the unitarity relation $\text{Tr}[\rho_H] = 1$.

The relation in Eq. (3.8) provides a simple way to compute the polarization density matrix of the massive spin-1 particles starting from the amplitudes of the related production process. In the case of $V = W$, we find that the non-vanishing f_a elements are given as

$$\begin{aligned} f_3 &= -\frac{1}{6\Phi_H} \left[1 - f^2 (\tilde{a}_V^2 + a_V^2) \right] \Delta_H, \\ f_8 &= -\frac{1}{\sqrt{3}} f_3, \end{aligned} \quad (3.10)$$

¹For the helicity basis we use a representation where the eigenstates of S_3 read

$$|+\rangle = \begin{pmatrix} 1 \\ 0 \\ 0 \end{pmatrix}, \quad |0\rangle = \begin{pmatrix} 0 \\ 1 \\ 0 \end{pmatrix}, \quad |-\rangle = \begin{pmatrix} 0 \\ 0 \\ 1 \end{pmatrix}, \quad (3.7)$$

corresponding to the eigenvalues $\lambda = +1, 0, -1$, respectively, and the symbols $(S_i)_{\lambda\lambda'}$ and $(S_{ij})_{\lambda\lambda'}$ are the corresponding matrix elements of the matrices S_i and S_{ij} on this basis respectively.

with $g_a = f_a$ for $a \in \{1, \dots, 8\}$, and where

$$\begin{aligned}\Phi_H &= \left[1 + 2f^2(\tilde{a}_V^2 + a_V^2)\right] m_H^4 - 2\left[1 + f^2(1 + 2\tilde{a}_V^2 + 2a_V^2 - 6a_V)\right] \\ &\quad + 2f^4(\tilde{a}_V^2 + a_V^2) m_H^2 M_V^2 + \left[1 + 2f^6(\tilde{a}_V^2 + a_V^2)\right. \\ &\quad \left. + 2f^2(5 + \tilde{a}_V^2 + a_V^2 - 6a_V) + f^4(1 - 4\tilde{a}_V^2 + 8a_V^2 - 12a_V)\right] M_V^4\end{aligned}\quad (3.11)$$

and

$$\Delta_H = \left[m_H^4 - 2(1 + f^2) m_H^2 M_V^2 + (1 - f^2)^2 M_V^4\right]. \quad (3.12)$$

The non-vanishing $h_{ab} = \tilde{h}_{ab}/\Phi_H$ elements for $V = W$ are given as

$$\begin{aligned}\tilde{h}_{16} &= -\frac{1}{2}f\left\{a_V m_H^2 - \left[(1 + f^2)a_V - 2\right]M_V^2\right\}\left\{m_H^2 - \left[1 + f^2(1 - 2a_V)\right]M_V^2\right\}, \\ \tilde{h}_{61} &= \tilde{h}_{16} = \tilde{h}_{27} = \tilde{h}_{72}, \\ \tilde{h}_{17} &= -\frac{1}{2}f\tilde{a}_V\left\{m_H^2 - \left[1 + f^2(1 - 2a_V)\right]M_V^2\right\}\sqrt{\Delta_H}, \\ \tilde{h}_{71} &= -\tilde{h}_{17} = \tilde{h}_{26} = -\tilde{h}_{62}, \\ \tilde{h}_{45} &= f^2\tilde{a}_V\left\{a_V m_H^2 + \left[2 - (1 + f^2)a_V\right]M_V^2\right\}\sqrt{\Delta_H}, \\ \tilde{h}_{54} &= -\tilde{h}_{45}, \\ \tilde{h}_{33} &= \frac{1}{4}\left\{m_H^2 - \left[1 + f^2(1 - 2a_V)\right]M_V^2\right\}^2, \\ \tilde{h}_{38} &= \tilde{h}_{83} = -\frac{1}{4\sqrt{3}}\Phi_H, \\ \tilde{h}_{44} &= \tilde{h}_{55} = \frac{1}{2}f^2\left\{\left[a_V m_H^2 + 2M_V^2 - (1 + f^2)a_V M_V^2\right]^2 - \tilde{a}_V^2 \Delta_H\right\}, \\ \tilde{h}_{88} &= \frac{1}{12}\left\{\left[1 - 4f^2(\tilde{a}_V^2 + a_V^2)\right]m_H^4 - 2\left[1 + f^2(1 - 4\tilde{a}_V^2 - 4a_V^2 + 6a_V) - 4f^4(\tilde{a}_V^2 + a_V^2)\right]m_H^2 M_V^2\right. \\ &\quad \left.+ \left[1 - 2f^2(7 + 2\tilde{a}_V^2 + 2a_V^2 - 6a_V) + f^4(1 + 8\tilde{a}_V^2 - 4a_V^2 + 12a_V) - 4f^6(\tilde{a}_V^2 + 2a_V^2)\right]M_V^4\right\}.\end{aligned}\quad (3.13)$$

The dependence of the polarization entanglement on the mass of the virtual state is due to the contribution of the longitudinal polarization. At threshold it yields a singlet state and the maximum of entanglement. Analogous results hold in the case of the $V = Z$ case, with the appropriate replacement of the anomalous couplings and SM coefficient ξ_Z .

The density matrix for the Higgs decay, as embodied by the coefficients in Eqs. (3.10)–(3.13), describes a pure state, that is $\rho_H^2 = \rho_H$, in the SM [2, 4] and after adding the anomalous couplings as well. This remarkable fact follows from the state being, so to speak, prepared by the formation of the spin-0 decaying particle which turns a generic mixed state (as that produced by colliding protons) into a pure one. This state can be written as

$$|\Psi\rangle = \frac{1}{|\overline{\mathcal{M}}|}\left[h_+ |V(+)V^*(-)\rangle + h_0 |V(0)V^*(0)\rangle + h_- |V(-)V^*(+)\rangle\right], \quad (3.14)$$

with

$$|\overline{\mathcal{M}}|^2 = |h_0|^2 + |h_+|^2 + |h_-|^2, \quad (3.15)$$

where the helicity amplitudes h_λ are defined in Eq. (2.7).

The relative weight of the transverse components $|V(+)\mathcal{V}^*(-)\rangle$ and $|V(-)\mathcal{V}^*(+)\rangle$ with respect to the longitudinal one $|V(0)\mathcal{V}^*(0)\rangle$ is controlled by the conservation of angular momentum. In general, only the helicity is conserved and the state in Eq. (3.14) belongs to the $J_z = 0$ component of either the $J = 0, 1$ or 2 states or a linear combination of them. For the SM model Higgs, for which $h_- = h_+$, the pure state in Eq. (3.14) is given by

$$|\Psi\rangle = \frac{1}{\sqrt{2 + \varkappa^2}} \left[|V(+)\mathcal{V}^*(-)\rangle - \varkappa |V(0)\mathcal{V}^*(0)\rangle + |V(-)\mathcal{V}^*(+)\rangle \right]. \quad (3.16)$$

with $\varkappa = 1 + (m_H^2 - (1+f)^2 M_V^2)/(2fM_V^2)$ [4]. The state in Eq. (3.16) is the singlet state when $\varkappa = 1$ —which happens if the final vector bosons are produced at rest.

After making the Kronecker product in Eq. (3.8) explicit, the resulting 9×9 polarization density matrix $\rho = |\Psi\rangle\langle\Psi|$ is written as

$$\rho_H = \frac{1}{|\mathcal{M}|^2} \begin{pmatrix} 0 & 0 & 0 & 0 & 0 & 0 & 0 & 0 & 0 \\ 0 & 0 & 0 & 0 & 0 & 0 & 0 & 0 & 0 \\ 0 & 0 & h_+ h_+^* & 0 & h_+ h_0^* & 0 & h_+ h_-^* & 0 & 0 \\ 0 & 0 & 0 & 0 & 0 & 0 & 0 & 0 & 0 \\ 0 & 0 & h_0 h_+^* & 0 & h_0 h_0^* & 0 & h_0 h_-^* & 0 & 0 \\ 0 & 0 & 0 & 0 & 0 & 0 & 0 & 0 & 0 \\ 0 & 0 & h_- h_+^* & 0 & h_- h_0^* & 0 & h_- h_-^* & 0 & 0 \\ 0 & 0 & 0 & 0 & 0 & 0 & 0 & 0 & 0 \\ 0 & 0 & 0 & 0 & 0 & 0 & 0 & 0 & 0 \end{pmatrix}, \quad (3.17)$$

in which, in terms of the anomalous couplings in Eq. (1.1), we have

$$\begin{aligned} h_0 &= -Ax - B(x^2 - 1), \\ h_\pm &= A \mp C\sqrt{x^2 - 1}. \end{aligned} \quad (3.18)$$

The coefficients A and B for $V = W$ are given by

$$\begin{aligned} A &= g \left(M_V + a_V \frac{k_1 \cdot k_2}{M_V} \right) \\ B &= -g a_V M_V, \quad C = ig \tilde{a}_V M_V \end{aligned} \quad (3.19)$$

with $x = m_H^2/(2fM_V^2) - (f^2 + 1)/(2f)$. The amplitudes entering the density matrix in Eq. (3.17) can be written in terms of the f_a, g_a, h_{ab} coefficients in the Gell-Mann basis as

$$\begin{aligned} \hat{h}_- \hat{h}_-^* &= \frac{1}{9} \left[1 + 3\sqrt{3} (f_8 - 2g_8 - 2h_{38}) + 9f_3 - 6h_{88} \right], \\ \hat{h}_0 \hat{h}_-^* &= h_{16} + i (h_{17} - h_{26}) + h_{27}, \\ \hat{h}_+ \hat{h}_-^* &= h_{44} + i (h_{45} - h_{54}) + h_{55}, \\ \hat{h}_0 \hat{h}_0^* &= \frac{1}{9} \left[1 - 9(f_3 + g_3 - h_{33}) + 3\sqrt{3} (f_8 + g_8 - h_{38} - h_{83}) + 3h_{88} \right], \\ \hat{h}_+ \hat{h}_0^* &= h_{61} + i (h_{62} - h_{71}) + h_{72}, \\ \hat{h}_+ \hat{h}_+^* &= \frac{1}{9} \left[1 + 3\sqrt{3} (g_8 - 2f_8 - 2h_{83}) + 9g_3 - 6h_{88} \right], \end{aligned} \quad (3.20)$$

where $\hat{h}_\lambda \equiv h_\lambda/|\overline{\mathcal{M}}|$. Eq. (3.20) makes it possible to go from the Gell-Mann basis to that of the helicities. In the limit of vanishing anomalous couplings, the results in Eqs.(3.10)-(3.13) go into those corresponding to the SM [4].

The main theoretical uncertainty affecting the correlation coefficients in Eqs. (3.10)–(3.13) is due to higher order corrections to the tree-level values. To estimate the size of these contributions, we take as guidance the results in [39, 40]—in which the NLO corrections have been computed—and assume that the error induced by these missing corrections yields approximately 1% of uncertainty on the main entanglement observables in the relevant kinematic regions.

Having determined the entries in the density matrix, we now study the dependencies of the observable introduced in the previous Section on the anomalous couplings.

- As mentioned before, the decays of the Higgs boson lead to the production of bipartite polarization states that are pure. When neglecting the background processes we can then use the entropy of entanglement to measure the entanglement among the polarizations of the massive gauge bosons. Only a_V enters linearly in \mathcal{E}_{ent} ; the coupling \tilde{a}_V by itself only enters quadratically. We do not write out the explicit expression of this operator because it is cumbersome (involving, as it does, the eigenvalues necessary in the definition of the logarithm of a matrix);
- The leading dependence of the observable \mathcal{C}_{odd} is linear in \tilde{a}_V . The anomalous couplings a_V only enters in \mathcal{C}_{odd} multiplied by \tilde{a}_V and is therefore quadratically suppressed. Utilizing the coefficients in Eqs. (3.10)–(3.13), the observable is given by

$$\mathcal{C}_{odd} = \frac{\tilde{a}_V f(1 + a_V f)\sqrt{\Delta_H}}{\Phi_H} \left\{ m_H^2 + (1 - f)^2 M_V^2 \right\}. \quad (3.21)$$

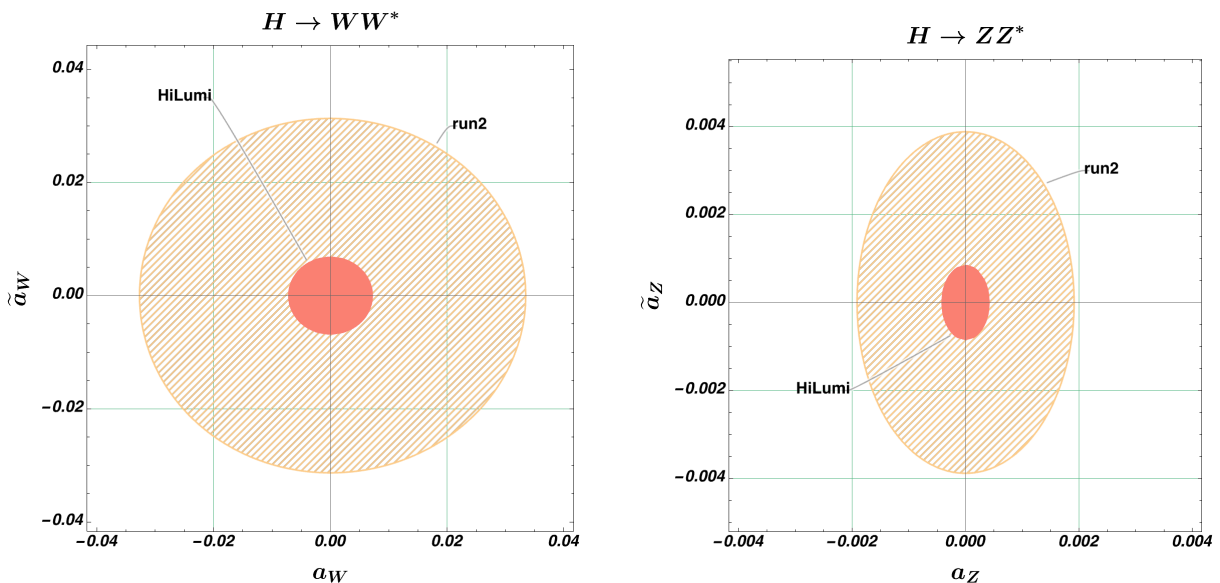


Figure 3: Allowed values for the anomalous couplings a_V and \tilde{a}_V obtained by using the observables \mathcal{C}_{odd} and \mathcal{E}_{ent} . The hatched area use the LHC run2 data ($\mathcal{L} = 140 \text{ fb}^{-1}$), the purple ones show the HiLumi projection ($\mathcal{L} = 3 \text{ ab}^{-1}$). The limits, all given at a 95% confidence level, only hold prior to the inclusion of backgrounds.

The two observables \mathcal{E}_{ent} and \mathcal{C}_{odd} seem to be ideal inasmuch as each of them depends linearly on one of the anomalous couplings while marginalizing the other. Cross dependencies are quadratic and very small in the range of values we consider.

The two observables depend on the mass of the off-shell gauge bosons, parametrized by fM_W . We have taken their average value by integrating over the parameter f within its limits to obtain the

<i>LHC</i>	<i>run2</i>	<i>HiLumi</i>
	$ a_W \leq 0.033$	$ a_W \leq 0.0070$
	$ \tilde{a}_W \leq 0.031$	$ \tilde{a}_W \leq 0.0068$
	$ a_Z \leq 0.0019$	$ a_Z \leq 0.00040$
	$ \tilde{a}_Z \leq 0.0039$	$ \tilde{a}_Z \leq 0.00086$

Table 1: 95% confidence intervals for the anomalous couplings obtained by marginalization of the two-parameter plots in Fig. 3. when taken to be independent.

results shown in Fig. 3. The limits for the Hi-Lumi case are obtained by rescaling the uncertainties by the square root of the ratio of the luminosities $\sqrt{300/14}$. The limits on single anomalous couplings, presented in Tab. 1, are obtained by marginalization of the other one.

To put our result in perspective, we can compare it to the only theoretical estimate [28] which is based, as ours, on observables derived from the polarizations (but not the entanglement). They find

$$a_Z = 6.88 \times 10^{-3}, \quad \tilde{a}_Z = 9.53 \times 10^{-3} \quad (3.22)$$

at 1σ , in the linear approximation, and for a luminosity of 1 ab^{-1} , whereas, for HiLumi (3 ab^{-1}), we find (95% CL)

$$a_Z = 4.0 \times 10^{-4}, \quad \tilde{a}_Z = 8.0 \times 10^{-4}. \quad (3.23)$$

Beside the different statistical distribution and luminosities used, our result is stronger than the former limits obtained for the associated HZ production process. The limits in Eq. (3.23) are so stringent to be comparable with projected bounds from future lepton colliders [41–43] based on classical spin correlations and cross sections.

Although the use of entanglement does seem to strengthen the constraints on the anomalous couplings, we must include the effect of the backgrounds for a more realistic estimate of its power.

3.1 Including the background

The estimate of the dominant W plus jets background for the $H \rightarrow WW^*$ case is currently affected by a rather large uncertainty and its size is larger than the signal. Although we could in principle apply our method, the computation of this background is much more involved and it will require a dedicated simulation, which is outside the scope of the present analysis.

In the following we focus on the ZZ^* decay that achieves higher sensitivity to the anomalous couplings because of a better signal-to-background ratio than the WW^* case.

The irreducible background for the $H \rightarrow Z\ell^+\ell^-$ signal is rather small and dominated by the electroweak process $pp \rightarrow ZZ/Z\gamma \rightarrow 4\ell$. The sum of the signal and background, being induced by different production channels, is characterized by a mixture of different states. We introduce this mixture by writing the density matrices for the processes as

$$\rho_{ZZ} = \alpha\rho_{H \rightarrow ZZ} + (1 - \alpha)\rho_{\text{BCKG}}, \quad (3.24)$$

with $0 \leq \alpha \leq 1$ parametrizing the expected signal-to-background ratio $S/(S+B)$. The density matrix ρ_{BCKG} in Eq. (3.24) is given by the electroweak $pp \rightarrow ZZ$ process. We take $\alpha = 0.8$, corresponding to a background which is about 4 times smaller than the signal, which is the case at the Higgs peak [44].

Once the background is included, we can no longer use the entropy to measure the entanglement as the produced bipartite state is not pure. We use the observable \mathcal{C}_2 instead, which still tracks the

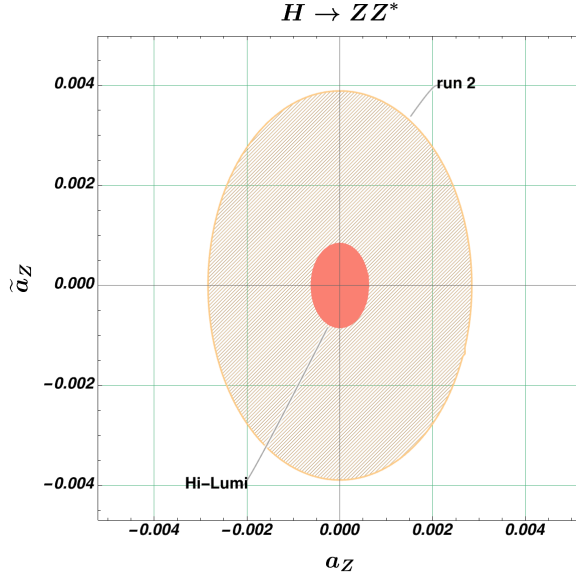


Figure 4: The same limits as in Fig. 3 (LHC run2 and HiLumi projections) as obtained for the ZZ^* channel after the inclusion of background. The observables \mathcal{C}_2 and \mathcal{C}_{odd} are used in this case.

<i>LHC</i>	<i>run2</i>	<i>HiLumi</i>
	$ a_Z \leq 0.0028$	$ a_Z \leq 0.00062$
	$ \tilde{a}_Z \leq 0.0039$	$ \tilde{a}_Z \leq 0.00086$

Table 2: 95% confidence intervals for the anomalous couplings obtained by marginalization of the two-parameter plots in Fig. 4. when taken to be independent.

entanglement, decreasing as the latter weakens. The observable \mathcal{C}_{odd} does not receive any contribution from the backgrounds, which are CP even.

4 Outlook

WE HAVE OUTLINED A STRATEGY to improve the current constraints on the anomalous couplings of the Higgs boson to the weak gauge bosons by means of the quantum tomography of the Higgs boson decay.

When comparing the limits found for the $H \rightarrow ZZ^*$ process in presence of background processes to those reported by the CMS collaboration one has to write them, in terms of the parameters f_{g2} and f_{g3} introduced in [17], as

$$f_{g2} = \frac{\sigma_2}{\sigma} |a_V|^2, \quad \text{and} \quad f_{g3} = \frac{\sigma_3}{\sigma} |\tilde{a}_V|^2, \quad (4.1)$$

where we take all anomalous coupling to be real and σ_i is the cross section in which only the corresponding coupling is included, σ the total cross section with all couplings included. Taking the values in Tab. 2, we have for run2 at the LHC

$$f_{g2}^Z < 7.8 \times 10^{-6}, \quad f_{g3}^Z < 1.5 \times 10^{-5}, \quad (4.2)$$

which can be compared to the best current experimental bounds from the CMS collaboration [29]:

$$f_{g2}^V < 3.4 \times 10^{-3}, \quad f_{g3}^V < 1.4 \times 10^{-2}, \quad (4.3)$$

obtained by using a combination of cross sections, including production ones, for processes where the HZZ vertices are identified. A comparison of the limits thus found with those of the experimental collaboration shows how well the proposed set of observables perform. In comparing, one must bear in mind that our limits come from a single process while those with which we compare come from the simultaneous use of more cross sections. On the other hand, our limits are mostly idealized whereas those from the experimental collaborations come with a full estimate of the statistical and systematic uncertainties as well as the actual backgrounds.

It goes without saying that all the limits we quote depend on the uncertainty in the analysis (about which we have made an educated guess) and that they can become stronger or weaker depending on how well (or badly) the actual physical analysis will turn out to be. In this respect, the main purpose of the present analysis is to highlight the potential of the new observables in constraining the anomalous couplings. In this light, we proved that their inclusion in routine analyses could lead to more stringent limits from global fits, which are currently based only on cross sections.

Acknowledgements

L.M. is supported by the Estonian Research Council grant PRG356.

References

- [1] A. J. Barr, *Testing Bell inequalities in Higgs boson decays*, *Phys. Lett. B* **825** (2022) 136866, [[arXiv:2106.01377](#)].
- [2] J. A. Aguilar-Saavedra, A. Bernal, J. A. Casas, and J. M. Moreno, *Testing entanglement and Bell inequalities in $H \rightarrow ZZ$* , *Phys. Rev. D* **107** (2023), no. 1 016012, [[arXiv:2209.13441](#)].
- [3] R. Ashby-Pickering, A. J. Barr, and A. Wierzychucka, *Quantum state tomography, entanglement detection and Bell violation prospects in weak decays of massive particles*, *JHEP* **05** (2023) 020, [[arXiv:2209.13990](#)].
- [4] M. Fabbrichesi, R. Floreanini, E. Gabrielli, and L. Marzola, *Bell inequalities and quantum entanglement in weak gauge bosons production at the LHC and future colliders*, [arXiv:2302.00683](#).
- [5] R. Horodecki, P. Horodecki, M. Horodecki, and K. Horodecki, *Quantum entanglement*, *Rev. Mod. Phys.* **81** (2009) 865–942, [[quant-ph/0702225](#)].
- [6] J. S. Bell, *On the einstein podolsky rosen paradox*, *Physics Physique Fizika* **1** (Nov, 1964) 195–200.
- [7] A. Soni and R. M. Xu, *Probing CP violation via Higgs decays to four leptons*, *Phys. Rev. D* **48** (1993) 5259–5263, [[hep-ph/9301225](#)].
- [8] D. Chang, W.-Y. Keung, and I. Phillips, *CP odd correlation in the decay of neutral Higgs boson into $Z Z$, $W^+ W^-$, or t anti- t* , *Phys. Rev. D* **48** (1993) 3225–3234, [[hep-ph/9303226](#)].
- [9] A. Skjold and P. Osland, *Angular and energy correlations in Higgs decay*, *Phys. Lett. B* **311** (1993) 261–265, [[hep-ph/9303294](#)].
- [10] C. P. Buszello, I. Fleck, P. Marquard, and J. J. van der Bij, *Prospective analysis of spin- and CP-sensitive variables in $H \rightarrow Z Z \rightarrow l(1)^+ l(1)^- l(2)^+ l(2)^-$ at the LHC*, *Eur. Phys. J. C* **32** (2004) 209–219, [[hep-ph/0212396](#)].
- [11] S. Y. Choi, D. J. Miller, M. M. Muhlleitner, and P. M. Zerwas, *Identifying the Higgs spin and parity in decays to Z pairs*, *Phys. Lett. B* **553** (2003) 61–71, [[hep-ph/0210077](#)].
- [12] Y. Gao, A. V. Gritsan, Z. Guo, K. Melnikov, M. Schulze, and N. V. Tran, *Spin Determination of Single-Produced Resonances at Hadron Colliders*, *Phys. Rev. D* **81** (2010) 075022, [[arXiv:1001.3396](#)].
- [13] N. D. Christensen, T. Han, and Y. Li, *Testing CP Violation in ZZH Interactions at the LHC*, *Phys. Lett. B* **693** (2010) 28–35, [[arXiv:1005.5393](#)].
- [14] N. Desai, D. K. Ghosh, and B. Mukhopadhyaya, *CP-violating HWW couplings at the Large Hadron Collider*, *Phys. Rev. D* **83** (2011) 113004, [[arXiv:1104.3327](#)].
- [15] S. Bolognesi, Y. Gao, A. V. Gritsan, K. Melnikov, M. Schulze, N. V. Tran, and A. Whitbeck, *On the spin and parity of a single-produced resonance at the LHC*, *Phys. Rev. D* **86** (2012) 095031, [[arXiv:1208.4018](#)].
- [16] S. Dwivedi, D. K. Ghosh, B. Mukhopadhyaya, and A. Shivaji, *Distinguishing CP-odd couplings of the Higgs boson to weak boson pairs*, *Phys. Rev. D* **93** (2016) 115039, [[arXiv:1603.06195](#)].
- [17] I. Anderson et al., *Constraining Anomalous HVV Interactions at Proton and Lepton Colliders*, *Phys. Rev. D* **89** (2014), no. 3 035007, [[arXiv:1309.4819](#)].
- [18] P. Artoisenet et al., *A framework for Higgs characterisation*, *JHEP* **11** (2013) 043, [[arXiv:1306.6464](#)].
- [19] S. Boselli, C. M. Carloni Calame, G. Montagna, O. Nicrosini, F. Piccinini, and A. Shivaji, *Higgs decay into four charged leptons in the presence of dimension-six operators*, *JHEP* **01** (2018) 096, [[arXiv:1703.06667](#)].
- [20] I. Brivio, T. Corbett, and M. Trott, *The Higgs width in the SMEFT*, *JHEP* **10** (2019) 056, [[arXiv:1906.06949](#)].
- [21] M. Hellmund and G. Ranft, *GAUGE VECTOR BOSON PAIR PRODUCTION AT anti-p p COLLIDER ENERGIES*, *Z. Phys. C* **12** (1982) 333.
- [22] J. S. Shim, S. Baek, and H. S. Song, *Polarization effects in electroweak vector boson productions*, *J. Korean Phys. Soc.* **29** (1996) 293–299, [[hep-ph/9510242](#)].
- [23] G. Mahlon and S. J. Parke, *Deconstructing angular correlations in $Z H$, $Z Z$, and $W W$ production at LEP-2*, *Phys. Rev. D* **58** (1998) 054015, [[hep-ph/9803410](#)].

- [24] Z. Bern et al., *Left-Handed W Bosons at the LHC*, *Phys. Rev. D* **84** (2011) 034008, [arXiv:1103.5445].
- [25] W. J. Stirling and E. Vryonidou, *Electroweak gauge boson polarisation at the LHC*, *JHEP* **07** (2012) 124, [arXiv:1204.6427].
- [26] E. Maina, *Vector boson polarizations in the decay of the Standard Model Higgs*, *Phys. Lett. B* **818** (2021) 136360, [arXiv:2007.12080].
- [27] E. Maina and G. Pelliccioli, *Polarized Z bosons from the decay of a Higgs boson produced in association with two jets at the LHC*, *Eur. Phys. J. C* **81** (2021), no. 11 989, [arXiv:2105.07972].
- [28] K. Rao, S. D. Rindani, and P. Sarmah, *Study of anomalous gauge-Higgs couplings using Z boson polarization at LHC*, *Nucl. Phys. B* **964** (2021) 115317, [arXiv:2009.00980].
- [29] CMS Collaboration, A. M. Sirunyan et al., *Measurements of the Higgs boson width and anomalous HVV couplings from on-shell and off-shell production in the four-lepton final state*, *Phys. Rev. D* **99** (2019), no. 11 112003, [arXiv:1901.00174].
- [30] F. Mintert and A. Buchleitner, *Observable entanglement measure for mixed quantum states*, *Phys. Rev. Lett.* **98** (Apr, 2007) 140505.
- [31] P. Rungta, V. Bužek, C. M. Caves, M. Hillery, and G. J. Milburn, *Universal state inversion and concurrence in arbitrary dimensions*, *Phys. Rev. A* **64** (Sep, 2001) 042315.
- [32] ATLAS Collaboration, *Measurements of Higgs boson production by gluon-gluon fusion and vector-boson fusion using $H \rightarrow WW^* \rightarrow e\nu\mu\nu$ decays in pp collisions at $\sqrt{s} = 13$ TeV with the ATLAS detector*, arXiv:2207.00338.
- [33] ATLAS Collaboration, G. Aad et al., *Higgs boson production cross-section measurements and their EFT interpretation in the 4ℓ decay channel at $\sqrt{s} = 13$ TeV with the ATLAS detector*, *Eur. Phys. J. C* **80** (2020), no. 10 957, [arXiv:2004.03447]. [Erratum: *Eur.Phys.J.C* **81**, 29 (2021), Erratum: *Eur.Phys.J.C* **81**, 398 (2021)].
- [34] F. Fabbri, J. Howarth, and T. Maurin, *Isolating semi-leptonic $H \rightarrow WW^*$ decays for Bell inequality tests*, arXiv:2307.13783.
- [35] ATLAS Collaboration, G. Aad et al., *Measurement of the Higgs boson mass in the $H \rightarrow ZZ^* \rightarrow 4\ell$ decay channel using 139 fb^{-1} of $\sqrt{s} = 13$ TeV pp collisions recorded by the ATLAS detector at the LHC*, *Phys. Lett. B* **843** (2023) 137880, [arXiv:2207.00320].
- [36] CMS Collaboration, A. Tumasyan et al., *Measurements of the Higgs boson production cross section and couplings in the W boson pair decay channel in proton-proton collisions at $\sqrt{s} = 13$ TeV*, *Eur. Phys. J. C* **83** (2023), no. 7 667, [arXiv:2206.09466].
- [37] H. S. Song, *A Treatment of Spin 1 Polarization*, *Lett. Nuovo Cim.* **25** (1979) 161.
- [38] S. Y. Choi, T. Lee, and H. S. Song, *Density Matrix for Polarization of High Spin Particles*, *Phys. Rev. D* **40** (1989) 2477.
- [39] S. Actis, *NLO Electroweak Corrections to Higgs Decay to Two Photons*, in *International Linear Collider Workshop (LCWS08 and ILC08)*, 1, 2009. arXiv:0901.4681.
- [40] S. Boselli, C. M. Carloni Calame, G. Montagna, O. Nicrosini, and F. Piccinini, *Higgs boson decay into four leptons at NLOPS electroweak accuracy*, *JHEP* **06** (2015) 023, [arXiv:1503.07394].
- [41] T. Han and J. Jiang, *CP violating Z Z H coupling at $e^+ e^-$ linear colliders*, *Phys. Rev. D* **63** (2001) 096007, [hep-ph/0011271].
- [42] N. Craig, J. Gu, Z. Liu, and K. Wang, *Beyond Higgs Couplings: Probing the Higgs with Angular Observables at Future $e^+ e^-$ Colliders*, *JHEP* **03** (2016) 050, [arXiv:1512.06877].
- [43] P. Sharma and A. Shivaji, *Probing non-standard HVV ($V = W, Z$) couplings in single Higgs production at future electron-proton collider*, *JHEP* **10** (2022) 108, [arXiv:2207.03862].
- [44] CMS Collaboration, A. M. Sirunyan et al., *Measurements of production cross sections of the Higgs boson in the four-lepton final state in proton-proton collisions at $\sqrt{s} = 13$ TeV*, *Eur. Phys. J. C* **81** (2021), no. 6 488, [arXiv:2103.04956].